

# Comparison of the quantitative measurement of $^{18}\text{F}$ -FDG PET/CT and histopathological findings in IgG4-related disease

S. Tsuji<sup>1</sup>, N. Iwamoto<sup>1</sup>, Y. Horai<sup>2</sup>, K. Fujikawa<sup>3</sup>, Y. Fujita<sup>1</sup>, S. Fukui<sup>1</sup>, R. Ideguchi<sup>4</sup>, T. Michitsuji<sup>1</sup>, S. Nishihata<sup>1</sup>, M. Okamoto<sup>1</sup>, Y. Tsuji<sup>1</sup>, Y. Endo<sup>1</sup>, T. Shimizu<sup>1</sup>, R. Sumiyoshi<sup>1</sup>, T. Koga<sup>1,5</sup>, S. Kawashiri<sup>1,6</sup>, T. Igawa<sup>1</sup>, K. Ichinose<sup>1</sup>, M. Tamai<sup>1</sup>, H. Nakamura<sup>1</sup>, T. Origuchi<sup>7</sup>, T. Kudo<sup>4</sup>, A. Kawakami<sup>1</sup>

<sup>1</sup>Department of Immunology and Rheumatology, Division of Advanced Preventive Medical Sciences, Nagasaki University Graduate School of Biomedical Sciences, Nagasaki, Japan; <sup>2</sup>Department of Rheumatology, National Hospital Organization Nagasaki Medical Center, Omura, Japan; <sup>3</sup>Department of Rheumatology, Japan Community Healthcare Organization, Isahaya General Hospital, Isahaya, Japan; <sup>4</sup>Department of Radioisotope Medicine, Atomic Bomb Disease Institute, Nagasaki University, Nagasaki, Japan; <sup>5</sup>Center for Bioinformatics and Molecular Medicine, Nagasaki University Graduate School of Biomedical Sciences, Nagasaki, Japan; <sup>6</sup>Department of Community Medicine, Division of Advanced Preventive Medical Sciences, Nagasaki University Graduate School of Biomedical Sciences, Nagasaki, Japan; <sup>7</sup>Department of Physical Therapy, Nagasaki University Graduate School of Biomedical Sciences, Nagasaki, Japan.

## Abstract

### Objective

To investigate the utility of  $^{18}\text{F}$ -FDG PET/CT in the diagnostic procedure of IgG4-related disease (IgG4-RD), we analysed the association between quantitative method of  $^{18}\text{F}$ -FDG PET/CT and histological findings.

### Methods

Twenty-one patients with IgG4-RD in whom  $^{18}\text{F}$ -FDG PET/CT was performed at the time of diagnosis were enrolled. Tissue biopsy was performed at 24 sites in 21 patients. To perform quantitative analysis of  $^{18}\text{F}$ -FDG PET/CT imaging, the highest standardised uptake value (SUV) of the pixels ( $\text{SUV}_{\text{max}}$ ) and the average SUV ( $\text{SUV}_{\text{mean}}$ ) within the biopsied lesion were measured. The  $\text{SUV}_{\text{mean}}$  of the liver was also measured as a reference.

### Results

The mean age at diagnosis was  $64.6 \pm 11.9$  years, and the median serum IgG4 level was 650 mg/dl. Histological findings were consistent with IgG4-RD (histopathology-positive) at 19 out of 24 sites. Although there was no significant difference in the values of  $\text{SUV}_{\text{max}}$  between histopathology-positive and histopathology-negative tissues, the values of  $\text{SUV}_{\text{mean}}$  were significantly higher in the histopathology-positive tissue (4.98 and 3.54, respectively  $p < 0.05$ ). The values of  $\text{SUV}_{\text{mean}}/\text{liver}$  were also higher in the histopathology-positive tissue (2.17 and 1.52, respectively  $p < 0.05$ ). To establish a cut-off value of  $\text{SUV}_{\text{mean}}$  to determine which of multiple lesions should be biopsied, a ROC curve was constructed. ROC curve analysis indicated  $\text{SUV}_{\text{mean}} = 4.07$  or  $\text{SUV}_{\text{mean}}/\text{liver} = 1.66$  as a cut-off value.

### Conclusions

Our present study suggested that quantitative analysis of  $^{18}\text{F}$ -FDG-PET/CT imaging might be useful for selecting the biopsy site in IgG4-RD. The calculation of  $\text{SUV}_{\text{mean}}$ , not of  $\text{SUV}_{\text{max}}$ , is important for evaluating IgG4-RD-related lesions in  $^{18}\text{F}$ -FDG PET/CT imaging.

### Key words

IgG4-RD, PET/CT, standardised uptake value

Sosuke Tsuji, MD  
 Naoki Iwamoto, MD, PhD  
 Yoshiro Horai, MD, PhD  
 Keita Fujikawa, MD, PhD  
 Yuya Fujita, MD  
 Shoichi Fukui, MD, PhD  
 Reiko Ideguchi, MD, PhD  
 Toru Michitsuji, MD  
 Shinya Nishihata, MD  
 Momoko Okamoto, MD  
 Yoshika Tsuji, MD  
 Yushiro Endo, MD  
 Toshimasa Shimizu, MD, PhD  
 Remi Sumiyoshi, MD  
 Tomohiro Koga, MD, PhD  
 Shin-ya Kawashiri, MD, PhD  
 Takashi Igawa, MD  
 Kunhiro Ichinose, MD, PhD  
 Mami Tamai, MD, PhD  
 Hideki Nakamura, MD, PhD  
 Tomoki Origuchi, MD, PhD, Prof.  
 Takashi Kudo, MD, PhD, Prof.  
 Atsushi Kawakami, MD, PhD, Prof.

Please address correspondence to:

Naoki Iwamoto,  
 Department of Immunology  
 and Rheumatology, Division of  
 Advanced Preventive Medical Sciences,  
 Nagasaki University Graduate  
 School of Biomedical Sciences,  
 1-7-1 Sakamoto,  
 Nagasaki 852-8501, Japan.  
 E-mail: naoki-iwa@nagasaki-u.ac.jp

Received on August 11, 2020; accepted in  
 revised form on November 9, 2020.

© Copyright CLINICAL AND  
 EXPERIMENTAL RHEUMATOLOGY 2021.

Competing interests: none declared.

## Introduction

IgG4-related disease (IgG4-RD) is a systemic fibroinflammatory condition characterised by IgG4-positive plasma cell infiltration of the affected organs or tissue, resulting in organ enlargement and organ fibrosis (1, 2). The commonly affected organs are the lacrimal glands, salivary glands, periorbital tissue, pancreas, lymph nodes, retroperitoneal tissue, lung, kidney, and skin, and dysfunctions of these organs are sometimes a consequence of IgG4-RD (3, 4). The diagnosis of IgG4-RD is based on the combination of characteristic histopathologic, clinical, serologic, and radiologic findings (5, 6). IgG4-RD should also be differentiated from multiorgan disorders that may present organ enlargement, lymph node swelling, and tumour-like swelling, such as lymphoproliferative disease and neoplastic disease (6, 7).

It is thus important to biopsy the organ or tissue that is suspected to be affected by IgG4-RD, not only for diagnostic but also differential diagnostic purposes. However, until now, little has been known about the method of selecting the biopsy site from multiple suspected lesions. In addition, depending on the organ involved (e.g. the aorta or pituitary gland), a biopsy is sometimes a difficult and invasive procedure. A non-invasive method that can provide useful information for selecting a biopsy site that is suspected of being IgG4-RD-associated from among the lesions is therefore needed.

<sup>18</sup>F-fluoro-deoxyglucose positron emission tomography/computed tomography (<sup>18</sup>F-FDG PET/CT) is a functional imaging procedure that is widely used in the diagnosis, staging, treatment response, and relapse monitoring of various types of malignancies, including malignant lymphoma (8, 9). It can be a valuable tool in the workup of patients with newly diagnosed IgG4-RD, in particular for the detection of multiple-organ involvement (10-12). There is also accumulating evidence that <sup>18</sup>F-FDG uptake is correlated with the treatment response (10, 13, 14).

A quantitative analysis of PET parameters is an accurate, objective, and reproducible means of assessing PET im-

ages. The utility of the quantification of <sup>18</sup>F-FDG PET/CT for the differential diagnosis of patients clinically suspected of having IgG4-RD had been reported (15-17). In those studies, the <sup>18</sup>F-FDG uptake was lower in IgG4-RD than in malignancies (15, 16). However, the appropriate method of quantifying <sup>18</sup>F-FDG PET/CT may differ by disease, and a suitable method for use in IgG4-RD patients remains unknown. An appropriate method for quantification is needed to identify/investigate the IgG4-RD-associated lesions among multiple lesions by using the <sup>18</sup>F-FDG uptake and a semiquantitative method. Such a method would contribute to the selection of a biopsy site for diagnosis. Here, we evaluated the utility of quantifying <sup>18</sup>F-FDG PET/CT in the diagnosis of IgG4-RD by analysing the relationship between <sup>18</sup>F-FDG PET/CT findings and histopathologic findings. In addition, we determined the optimal method for the quantification of <sup>18</sup>F-FDG-PET/CT in IgG4-RD.

## Patients and methods

### Patients

Patients were recruited from the Department of Immunology and Rheumatology, Nagasaki University Graduate School of Biomedical Sciences, Isahaya General Hospital, and Nagasaki Medical Center. A total of 21 consecutive patients for whom <sup>18</sup>F-FDG PET/CT was undertaken at the time of diagnosis between November 2011 and July 2018 were enrolled. All patients fulfilled the comprehensive diagnostic criteria for IgG4-RD<sup>5</sup> and the 2019 American College of Rheumatology (ACR)/European League Against Rheumatism (EULAR) classification criteria for IgG4-RD (6). The decision whether to have the patient undergo <sup>18</sup>F-FDG PET/CT in order to exclude other diseases or to evaluate the organ involvement of IgG4-RD was made by each patient's treating physician with the agreement of the patient.

Tissue biopsies for at least one lesion with abnormal <sup>18</sup>F-FDG uptake were performed in all patients during the diagnostic procedure. The patients gave their informed consent to be subjected to the protocol, which was approved by

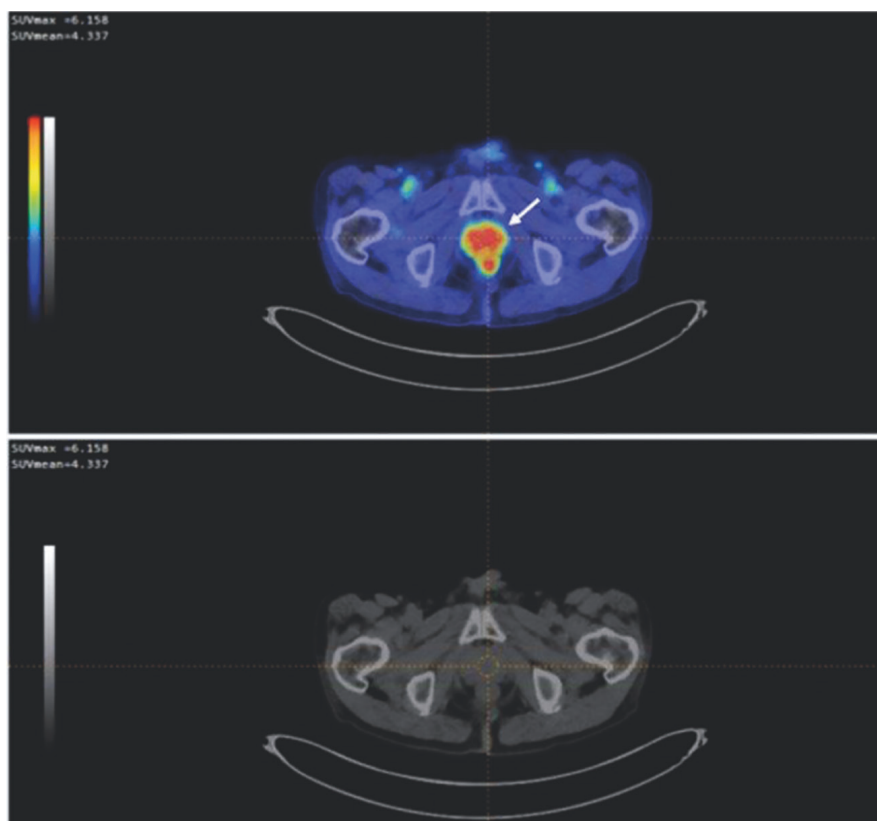


**Fig. 1.**  $^{18}\text{F}$ -FDG-PET imaging results of patients with IgG4-RD obtained with Metavol software. Upper panel: A fusion image of FDG and CT. The circle (white arrow) indicates the standardised uptake value (SUV)-measurement region. The colors indicate the level of FDG activity (red areas indicate high FDG activity). The prostate is showing strong uptake. Lower panel: A CT image of the same area.  $^{18}\text{F}$ -FDG-PET  $^{18}\text{F}$ -fluoro-2-deoxy-D-glucose positron emission tomography/computed tomography.

the Institutional Review Board (IRB) of Nagasaki University (IRB approval no.: 17091109).

We retrospectively reviewed the clinical, laboratory, and histopathological features and findings obtained by  $^{18}\text{F}$ -FDG PET/CT and evaluated the patients' clinical courses for 1 year.

#### Histopathological findings

Tissue biopsy was performed at the time of diagnosis. According to pathologic criteria for diagnosis of IgG4-RD proposed by the comprehensive diagnostic criteria for IgG4-RD and 2019 ACR/EULAR classification criteria for IgG4-RD (5, 6), we defined tissue that exhibited the following histopathological characteristics as histopathology-positive tissue: marked lymphocyte and plasmacytic infiltration with fibrosis, infiltration of IgG4-positive plasma cells with the ratio of IgG4+/IgG+ cells >40%, and an elevated number of IgG4+ plasma cells per high power field (>10).

#### $^{18}\text{F}$ -FDG PET/CT imaging

All patients underwent a  $^{18}\text{F}$ -FDG PET/CT scan on a dedicated PET/CT system (Siemens Biograph mCT, Germany, or Siemens Biograph 16true point, Germany, or GE Discovery ST, Wisconsin, USA) consisting of a PET scanner and a 64-row multidetector CT scanner. The patients fasted for more than 5 hours before the intravenous injection of  $^{18}\text{F}$ -FDG.  $^{18}\text{F}$ -FDG was injected intravenously at 180–325 MBq. One hour after the  $^{18}\text{F}$ -FDG injection, the scanning was performed from the middle of the thigh to the top of the skull. The CT data were used for calibration (attenuation correction).  $^{18}\text{F}$ -FDG uptake was assessed at the site of major organ involvement of IgG4-RD, which could be differentiated from the normal uptake of background tissue with  $^{18}\text{F}$ -FDG PET/CT.

#### Image analysis

For quantitative analysis, PET/CT images were extracted. We measured

the highest standardised uptake value (SUV) of the pixels ( $\text{SUV}_{\text{max}}$ ) and the average SUV ( $\text{SUV}_{\text{mean}}$ ) within the biopsied tissue using Metavol, which is a dedicated open-source software (Fig. 1) (18). We also measured the  $\text{SUV}_{\text{mean}}$  of the liver as a reference. We then calculated the ratio between the  $\text{SUV}_{\text{mean}}$  of the biopsied tissue and the  $\text{SUV}_{\text{mean}}$  of the liver ( $\text{SUV}_{\text{mean}}/\text{liver}$ ).

#### Statistical analyses

GraphPad prism software (GraphPad Software, San Diego, CA) and JMP Statistical Software (SAS Institute, Cary, NC) were used for the statistical analyses. We used the Kolmogorov-Smirnov test to check the normal distribution of the data, and an unpaired Student's t-test was used to detect significant differences in the SUV values. We constructed receiver operating characteristic (ROC) curves to establish the cut-off values of  $\text{SUV}_{\text{mean}}$  and  $\text{SUV}_{\text{mean}}/\text{liver}$  on which to base biopsy decisions. Probability ( $p$ )-values <0.05 were considered significant.

## Results

#### Baseline characteristics of the patients and disease course

The patients' characteristics are summarised in Table I. There were 21 patients (11 males, 10 females). The salivary gland and lymph node were the most commonly affected organs (71.4%), followed by the lacrimal gland (28.6%), pancreas (23.8%), retroperitoneum/abdominal aorta (19.0%), prostate (14.3%), and bile duct (4.8%). The median level of eosinophils was 250/ $\mu\text{l}$  (interquartile range, 183–392); C-reactive protein (CRP), 0.15 mg/dL (range, 0.05–0.3); IgE, 196.3 IU/mL (125.6–1254.6); and IgG4, 650 mg/dL (223.5–1075). The disease course of 11 patients could be analysed in this study. After the diagnosis of IgG4-RD, prednisolone treatment was initiated in all 21 patients, and there was no relapse for 1 year.

#### Quantitative $^{18}\text{F}$ -FDG PET/CT findings and histopathological findings

A tissue biopsy was performed at 24 sites (lymph node 4, submandibular gland 10, prostate gland 4, pancreas

2, thyroid gland 1, lung 1, retroperitoneum 1, and kidney 1) in the 21 patients. Among these 24 sites, 19 tissues were histopathology-positive; the histopathological findings for the other five tissues were not consistent with the pathologic criteria for the diagnosis of IgG4-RD (Table II). These five histopathology-negative tissues were also not consistent with other diseases such as malignant lymphoma. Almost all of these histopathological findings showed lymphocyte and plasmacytic infiltration with few or no IgG4-positive cells.

The values of SUV<sub>max</sub> and SUV<sub>mean</sub> for each organ and SUV<sub>mean</sub>/liver are provided in Table III. The IgG4-RD-involved organ with the highest SUV<sub>max</sub> was the lung, and the lowest was the retroperitoneum (7.61 and 3.37, respectively), and the same tendency was seen in the analysis of the SUV<sub>mean</sub> (6.04 and 3.06, respectively). However, in the analysis of the ratio between the SUV<sub>mean</sub> and SUV<sub>mean</sub>/liver values of the liver, the organ that showed the highest value was the lymph node, and the prostate showed the lowest value (2.48 and 1.43, respectively). These results indicate the superficial organs (lymph nodes, submandibular organs) showed higher SUV value and histopathology-positive rate. There were no significant differences in the values of SUV<sub>max</sub>, SUV<sub>mean</sub> and SUV<sub>mean</sub>/liver among the organs. The mean values of SUV<sub>max</sub>, SUV<sub>mean</sub>, SUV<sub>mean</sub>/liver in all sites were 5.26, 4.68 and 2.04, respectively.

*Comparison between <sup>18</sup>F-FDG uptake and histopathological findings*

We next examined whether the <sup>18</sup>F-FDG uptake was correlated with the histopathological findings. Although there was no significant difference in the value of SUV<sub>max</sub> between histopathology-positive and histopathology-negative tissues, the values of SUV<sub>mean</sub> were significantly higher in the histopathology-positive tissues (Fig. 2). The values of SUV<sub>mean</sub>/liver were also higher in those of the histopathology-positive group as compared to in the histopathology-negative tissue.

To calculate the cut-off value of SUV<sub>mean</sub> to determine which among multiple lesions is to be biopsied, we

**Table I.** Clinical characteristics of the study population.

Parameters	
Age at onset (years)	64.6 ± 11.9
Female, n (%)	10 (47.6)
Organ involvement, n (%)	
Lacrimal gland	6 (28.6)
Salivary gland	15 (71.4)
Lymph node	15 (71.4)
Pancreas	5 (23.8)
Bile duct	1 (4.8)
Prostate	3 (14.3)
Retroperitoneum/Abdominal aorta	4 (19.0)
Number of affected organs	3.6 ± 1.9
Serological features	
Eosinophils, (median [IQR])	250 [183-392]
CRP (mg/dL), (median [IQR])	0.15 [0.05-0.3]
IgE (IU/mL), (median [IQR])	196.3 [125.6-1254.6]
IgG4 (mg/dL), (median [IQR])	650 [223.5-1075]
IgG4/IgG ratio, (median [IQR])	0.24 [0.13-0.42]
sIL2R (U/ml), (median [IQR])	801 [465.3-1427.5]

Data are mean ± standard deviation (SD) unless otherwise indicated. IQR interquartile range. CRP: C-reactive protein; IgE: immunoglobulin E; IgG4: immunoglobulin G4; IgG: immunoglobulin G; sIL2R: soluble interleukin-2 receptor.

**Table II.** Biopsy sites and histopathological findings.

Biopsy site	Histopathology-positive	Histopathology-negative
Lymph node	4	0
Submandibular gland	9	1
Prostate	2	2
Pancreas	1	1
Thyroid	0	1
Lung	1	0
Retroperitoneum	1	0
Kidney	1	0

**Table III.** Biopsy sites and the value of standardised uptake value (SUV).

	SUV <sub>max</sub>	SUV <sub>mean</sub>	SUV <sub>mean</sub> /liver
Lymph node	5.68 ± 2.39	5.17 ± 2.07	2.48 ± 1.17
Submandibular gland	5.94 ± 1.45	5.32 ± 0.90	2.27 ± 0.41
Prostate	3.69 ± 1.21	3.26 ± 0.93	1.43 ± 0.44
Pancreas	4.83 ± 0.23	4.25 ± 0.61	1.71 ± 0.27
Thyroid	4.39	3.88	1.64
Lung	7.61	6.04	2.05
Retroperitoneum	3.37	3.06	1.47
Kidney	4.27	3.87	1.92
Total	5.26 ± 1.71	4.68 ± 1.36	2.04 ± 0.65

Data are mean ± standard deviation (SD). SUV<sub>mean</sub>/liver was the ratio between the SUV<sub>mean</sub> of the biopsied tissue and the SUV<sub>mean</sub> of the liver. SUV standardised uptake value.

constructed a ROC curve (Fig. 3A). Curves were drawn for the SUV<sub>mean</sub> and SUV<sub>mean</sub>/liver, and the areas under the curves (AUCs) were 0.81 and 0.82, respectively. According to the ROC curve analysis, at the best discriminative SUV<sub>mean</sub> cut-off of 4.07, the sensitivity and specificity were 79.0% and 80.0%, respectively. Moreover, the ROC curve analysis revealed SUV<sub>mean</sub>/liver = 1.66

to be the appropriate cut-off value with sensitivity and specificity of 84.2% and 80.0%, respectively (Fig. 3B).

**Discussion**

We investigated the relationship between the value of SUV on <sup>18</sup>F-FDG PET/CT imaging and the histopathological findings of suspected IgG4-RD-involved lesions. To avoid unnecessary

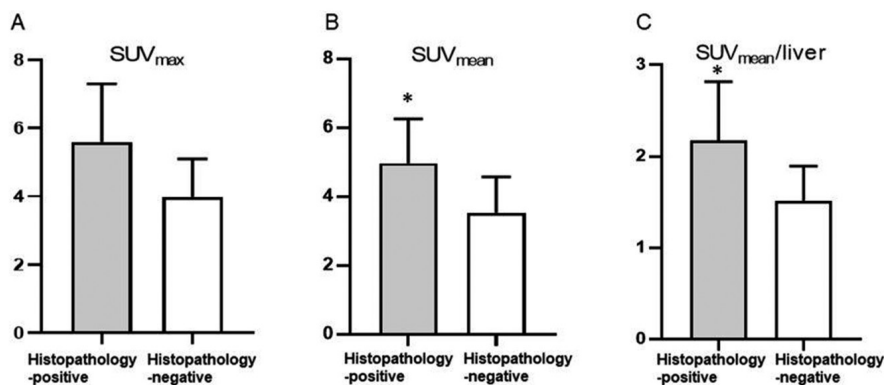


**Fig. 2.** The difference of the value of standardised uptake value (SUV) within the biopsied tissue. **A:** The values of  $\text{SUV}_{\text{max}}$  were no significant difference between histopathology-positive tissues (n=19) and histopathology-negative tissues (n=5). **B:** The value of  $\text{SUV}_{\text{mean}}$  were significantly higher in histopathology-positive tissues. **C:** The value of  $\text{SUV}_{\text{mean}}/\text{liver}$  were also significantly higher in histopathology-positive tissues. Values are presented as means  $\pm$  SD. \*  $p < 0.05$  vs. histopathology-negative tissues.

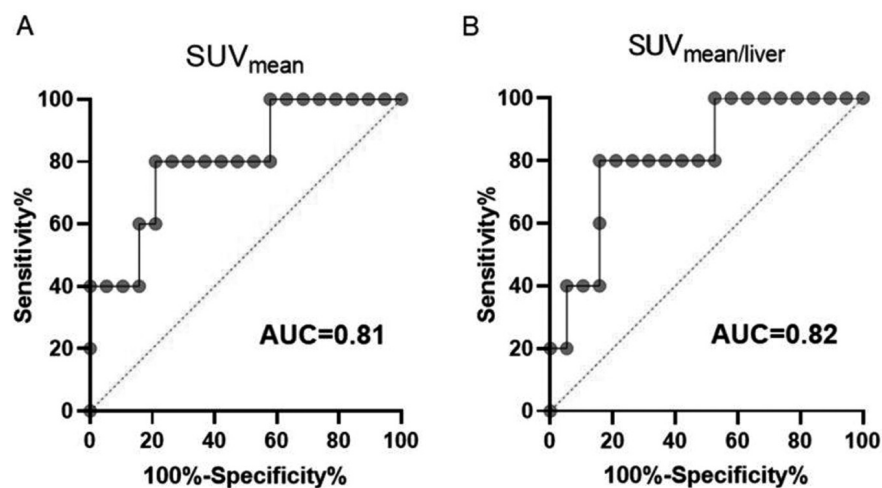


**Fig. 3.** Receiver operating characteristic (ROC) curve for determining which among multiple lesions is to be biopsied. **A:** ROC analysis for  $\text{SUV}_{\text{mean}}$  of biopsy lesions. **B:** ROC analysis for  $\text{SUV}_{\text{mean}}/\text{liver}$  of biopsy lesions. SUV standardised uptake value, AUC areas under the curve.

biopsies and to select suitable lesions for biopsy in diseases with multi-organ involvement such as IgG4-RD, it is important to determine which lesion is suspected to be disease-involved by using a non-invasive test. The results of our present analyses indicated that the value of the  $\text{SUV}_{\text{mean}}$ , but not the  $\text{SUV}_{\text{max}}$ , has good diagnostic performance in IgG4-RD.

In IgG4-RD,  $^{18}\text{F}$ -FDG PET/CT has been reported to be more accurate and more sensitive for detecting the lesions associated with IgG4-RD as compared to other imaging techniques. Zhang *et al.* reported  $^{18}\text{F}$ -FDG uptake in multiple organs in 34 of 35 IgG4-RD pa-

tients, and  $^{18}\text{F}$ -FDG PET/CT imaging was able to detect more organ involvements in 25 of 35 patients as compared to conventional evaluations including ultrasonography and conventional CT (12). Another report revealed that all 21 IgG4-RD patients who underwent  $^{18}\text{F}$ -FDG PET/CT presented  $^{18}\text{F}$ -FDG uptake in typical IgG4-RD localisations, and some of these lesions were not detected by conventional CT, magnetic resonance imaging, or ultrasound (10). Moreover, the correlation of disease activity and  $^{18}\text{F}$ -FDG PET/CT has also been reported (10, 13, 14).  $^{18}\text{F}$ -FDG uptake was seen in all patients enrolled in our present study, and sev-

eral lesions with  $^{18}\text{F}$ -FDG uptake were not detected by other imaging modalities (data not shown). Based on these previous studies, we further analysed whether the characteristics of the region of interest (ROI) of  $^{18}\text{F}$ -FDG PET/CT imaging correlated with true lesions of IgG4-RD by comparing them with histopathology. To analyse the characteristics of suspected IgG4-RD-involved lesions, quantitative analysis was performed. Additionally, to identify the optimal quantitative method for IgG4-RD, we also performed three methods of quantitative analysis. The optimal method for the quantification of PET/CT imaging might be different depending on the disease. For the differentiation of metastatic lesions of non-small-cell lung carcinoma from benign lymph nodes, the  $\text{SUV}_{\text{max}}$ -lymph node/ $\text{SUV}_{\text{max}}$ -primary tumour ratio showed better diagnostic performance as compared to  $\text{SUV}_{\text{max}}$ -lymph node (19, 20). Another study showed that the median SUV was correlated with local recurrence of squamous cell carcinoma of the anal canal but the  $\text{SUV}_{\text{mean}}$  was not correlated with local recurrence (21). In patients with head-and-neck cancer, the  $\text{SUV}_{\text{mean}}$ , and not the  $\text{SUV}_{\text{max}}$ , was correlated with disease-free survival, and thus the  $\text{SUV}_{\text{mean}}$  seemed to have the potential to become a prognostic factor in head-and-neck cancer (22).

Our present study showed that  $\text{SUV}_{\text{mean}}$  and  $\text{SUV}_{\text{mean}}/\text{liver}$  were significantly correlated with biopsy-proven IgG4-RD involvement, but that  $\text{SUV}_{\text{max}}$  was not correlated. This is consistent with the results of other studies. Zhan *et al.* reported that diffusely elevated  $^{18}\text{F}$ -FDG uptake in organs should be considered to be more likely to indicate IgG4-RD lesions as compared to a patchy/nodule uptake pattern (12). Diffused and enlarged tissues/organs are clinicopathologic characteristics of IgG4-RD (23, 24), such as in the following examples: 1) diffuse infiltration of sinonasal mucosa with an IgG4-positive plasmacytic infiltrate in IgG4-related chronic rhinosinusitis; 2) diffusely thickened gastric mucosa on endoscopy in IgG4-related gastritis; 3) diffusely enlarged sausage-shaped pancreas in autoimmune pancreatitis (considered to be on the

IgG4-RD spectrum); 4) homogenous thyroid gland enlargement in IgG4-related thyroiditis; and 5) diffuse kidney enlargement and diffuse immune complex deposition in the tubular basement membrane in IgG4-related kidney disease. These characteristics are also consistent with our study; namely, the comparison of  $SUV_{mean}$  between tissues with abundant IgG4-positive plasmacytes and tissues with few/no IgG4-positive plasmacytes in our study showed more significant differences as compared to the analysis of  $SUV_{max}$ .  $SUV_{max}$  is the most commonly used <sup>18</sup>F-FDG PET/CT parameter in daily clinical practice, and it is often included in imaging reports. It is simple and quick to measure, but  $SUV_{max}$  may not represent the status of ROI in IgG4-RD because its value is taken from a single voxel.  $SUV_{mean}$  within an ROI is supposed to represent disease status in IgG4-RD more precisely, as we found in this study; therefore, we should calculate  $SUV_{mean}$  to identify IgG4-RD lesions. Furthermore, according to ROC curve analysis, the AUC using the value of  $SUV_{mean}/liver$  was higher as compared to that using the value of  $SUV_{mean}$ . This suggested that  $SUV_{mean}$  was influenced by the individual hepatic metabolism, and  $SUV_{mean}/liver$  might be more preferable.

ROC curve analysis also indicated  $SUV_{mean}=4.07$  or  $SUV_{mean}/liver=1.66$  as the cut-off value that discriminated IgG4-RD-associated lesions. This value might be useful for selecting appropriate tissue for biopsy among multiple lesions that are suspected to be associated with IgG4-RD by <sup>18</sup>F-FDG uptake or to determine if an <sup>18</sup>F-FDG uptake lesion on which a biopsy cannot be performed is an IgG4-RD-associated lesion. However, this cut-off value should be interpreted with caution because the appropriate cut-off value might be different in each organ. For example, the SUVs in the prostate and pancreas were relatively low in our study, although the SUV values of those organs have been reported to be almost the same in normal subjects as compared to other organs (25, 26). The appropriate cut-off value for each organ should be identified by analysing a larger number of patients in the future.

Although there is a possibility that the SUV value is influenced by organs as described above, our results showed that superficial organs such as lymph nodes had a higher biopsy positive rate and SUV values. Considering this result, a biopsy of superficial organs should be aggressively performed (both for safety and to obtain the accurate diagnosis) in patients who are clinically suspected of having IgG4-RD with enlarged superficial organs.

Several limitations of this study must be mentioned. The number of patients was small, and the longitudinal analysis was not fully performed. We could evaluate the clinical course for one year in 11 out of 21 patients, but there were no relapses or progression of disease. We therefore could not compare the value of <sup>18</sup>F-FDG PET/CT at baseline with respect to the treatment response or disease progression. To make PET/CT imaging more useful for the management of treatment for IgG4-RD, analysis of the relation of the SUV value with the treatment course such as an inadequate response to steroid treatment, the rate of relapse and concomitant use of immunosuppressant desistance is needed in a larger longitudinal study. The values of  $SUV_{mean}$  of lymph node were relatively higher as compared to other tissues, and all histopathologic findings of lymph nodes were histopathology-positive in our present study. These results influenced the cut-off value in this study. The value of  $SUV_{mean}$  of histopathology-negative lymph node should be compared with that of histopathology-positive lymph node, and mentioned above in the discussion section, further analysis is needed of the cut-off value of  $SUV_{mean}$  focused on each organ using larger samples. Also, comparison of the  $SUV_{mean}$  of IgG4-RD with those of other diseases such as malignant lymphoma was not done in this study. The utility of the quantification of PET/CT for differentiating IgG4-RD from other diseases should be assessed in a future study.

### Conclusions

In conclusion, our present study suggested that quantitative analysis of <sup>18</sup>F-FDG PET/CT imaging is useful for selecting the biopsy site in IgG4-related

disease. The calculation of  $SUV_{mean}$ , not of  $SUV_{max}$ , is important for evaluating IgG4-RD lesions in <sup>18</sup>F-FDG PET/CT imaging.

### References

1. STONE JH, ZEN Y, DESHPANDE V: IgG4-related disease. *N Engl J Med* 2012; 366: 539-51.
2. KAMISAWA T, ZEN Y, PILLAI S, STONE JH: IgG4-related disease. *Lancet* 2015; 385: 1460-71.
3. TONE JH, KHOSROSHAHI A, DESHPANDE V *et al.*: Recommendations for the nomenclature of IgG4-related disease and its individual organ system manifestations. *Arthritis Rheum* 2012; 64: 3061-7.
4. KOIZUMI S, KAMISAWA T, KURUMA S *et al.*: Organ correlation in IgG4-related diseases. *J Korean Med Sci* 2015; 30: 743-8.
5. UMEHARA H, OKAZAKI K, MASAKI Y *et al.*: Comprehensive diagnostic criteria for IgG4-related disease (IgG4-RD), 2011. *Mod Rheumatol* 2012; 22: 21-30.
6. WALLACE ZS, NADEN RP, CHARI S *et al.*: The 2019 American College of Rheumatology/European League Against Rheumatism classification criteria for IgG4-related disease. *Ann Rheum Dis* 2020; 79: 77-87.
7. BLEDSOE JR, DELLA-TORRE E, ROVATI L, DESHPANDE V: IgG4-related disease; review of the histopathologic features, differential diagnosis, and therapeutic approach. *APMIS* 2018; 126: 459-76.
8. MALDONADO A, GONZALEZ-ALENDA FJ, ALONSO M, SIERRA JM: PET-CT in clinical oncology. *Clin Transl Oncol* 2007; 9: 494-505.
9. DING JJ, CHEN YL, ZHOU SH, ZHAO K: Positron emission tomography/computed tomography in the diagnosis, staging, and prognostic evaluation of natural killer/T-cell lymphoma. *J Int Med Res* 2018; 46: 4920-9.
10. EBBO M, GRADOS A, GUEDEI E *et al.*: Usefulness of 2-[<sup>18</sup>F]-fluoro-2-deoxy-D-glucose-positron emission tomography/computed tomography for staging and evaluation of treatment response in IgG4-related disease: a retrospective multicenter study. *Arthritis Care Res (Hoboken)* 2014; 66: 86-96.
11. NAKATANI K, NAKAMOTO Y, TOGASHI K: Utility of FDG PET/CT in IgG4-related systemic disease. *Clin Radiol* 2012; 67: 297-305.
12. ZHANG J, CHEN H, MA Y *et al.*: Characterizing IgG4-related disease with (1)(8)F-FDG PET/CT: a prospective cohort study. *Eur J Nucl Med Mol Imaging* 2014; 41: 1624-34.
13. MARTINEZ-PIPIENTA G, NORIEGA-ALVAREZ E, SIMO-PERDIGO M: Study of systemic disease IgG4. Usefulness of 2-[<sup>18</sup>F]-fluoro-2-deoxy-D-glucose-positron emission tomography/computed tomography for staging, selection of biopsy site, evaluation of treatment response and follow-up. *Eur J Rheumatol* 2017; 4:222-5.
14. HUANG HL, FONG W, PEH WM, NIRAJ KA, LAM WW: The Utility of FDG PET/CT in IgG4-Related Disease with a focus on coronary artery involvement. *Nucl Med Mol Imaging* 2018; 52: 53-61.

15. ZHAO Z, WANG Y, GUAN Z, JIN J, HUANG F, ZHU J: Utility of FDG-PET/CT in the diagnosis of IgG4-related diseases. *Clin Exp Rheumatol* 2016; 34: 119-25.
16. LEE J, HYUN SH, KIM S *et al.*: Utility of FDG PET/CT for differential diagnosis of patients clinically suspected of IgG4-related disease. *Clin Nucl Med* 2016; 41: e237-43.
17. BERTI A, DELLA-TORRE E, GALLIVANONE F *et al.*: Quantitative measurement of 18F-FDG PET/CT uptake reflects the expansion of circulating plasmablasts in IgG4-related disease. *Rheumatology (Oxford)* 2017; 56: 2084-92.
18. HIRATA K, KOBAYASHI K, WONG KP *et al.*: A semi-automated technique determining the liver standardized uptake value reference for tumor delineation in FDG PET-CT. *PLoS One* 2014; 9: e105682.
19. CHO J, CHOE JG, PAHK K *et al.*: Ratio of mediastinal lymph node SUV to primary tumor SUV in (18)F-FDG PET/CT for nodal staging in non-small-cell lung cancer. *Nucl Med Mol Imaging* 2017; 51: 140-6.
20. LEE AY, CHOI SJ, JUNG KP, PARK JS, LEE SM, BAE SK: Characteristics of metastatic mediastinal lymph nodes of non-small cell lung cancer on preoperative F-18 FDG PET/CT. *Nucl Med Mol Imaging* 2014; 48: 41-6.
21. JONES MP, HRUBY G, METSER U *et al.*: FDG-PET parameters predict for recurrence in anal cancer - results from a prospective, multicentre clinical trial. *Radiat Oncol* 2019; 14: 140.
22. HIGGINS KA, HOANG JK, ROACH MC *et al.*: Analysis of pretreatment FDG-PET SUV parameters in head-and-neck cancer: tumor SUVmean has superior prognostic value. *Int J Radiat Oncol Biol Phys* 2012; 82: 548-53.
23. OBIORAH IE, HENAO VELASQUEZ A, OZDEMIRLI M: The clinicopathologic spectrum of IgG4-related disease. *Balkan Med J* 2018; 35: 292-300.
24. SAEKI T, KAWANO M: IgG4-related kidney disease. *Kidney Int* 2014; 85: 251-7.
25. TAN LT, ONG KL: Semi-quantitative measurements of normal organs with variable metabolic activity on FDG PET imaging. *Ann Acad Med Singapore* 2004; 33: 183-5.
26. ZINCIRKESER S, SAHIN E, HALAC M, SAGER S: Standardized uptake values of normal organs on 18F-fluorodeoxyglucose positron emission tomography and computed tomography imaging. *J Int Med Res* 2007; 35: 231-6.